Using multi-temporal satellite images to evaluate the changes of vegetation index of land cover in Thai Binh Province

van Cu Pham, Chu Xuan Huy, Nguyen Thi Thuy Hang, Thapa R. B., Frederic Borne

3

Using Multi-temporal Satellite Images to Evaluate the Changes of Vegetation Index of Land Cover in Thai Binh Province

Pham Van Cu, Chu Xuan Huy, Nguyen Thi Thuy Hang, Rajesh Bahadur Thapa, Frédéric Borne

Satellite images highlight the existing situation and expected threats against environment. The integration of maps displaying vegetation and urban indices with statistic data on pig production allows us to make clear the relation between land cover changes and pig production development in Thai Binh.

Introduction

The spatial analysis introduced in this study contributes to identify the relationship between traditional agricultural practice and pig production activities at the provincial scale. Most of the studies carried out in the framework of our project used local statistic and cartographic data in accepting their heterogeneity in their reliability and their standards (see next chapters). Under this circumstance, the use of multi-temporal remotely sensed data will contribute to complete the lack of data in some cases and to provide another vision to understand the spatio-temporal evolution of the land cover in Thai Binh through a series of vegetation indices extracted from the images. The vegetation indices computed for the whole image are associated to communal administrative map of Thai Binh to create a time series of vegetation indices of each commune. The integration of maps displaying the vegetation indices with statistic data on pig production allows us to make clear the relation between land cover changes and pig production development in Thai Binh.

The current research aims to highlight the existing situation and expected threats against environment. This preliminary work will be the base for a decision making and strengthening tool for the Thai Binh's authorities in order to define urgently suitable technologies for land-use and investment planning, and to enforce the regulation considering environment. For this purpose, a series of multi-temporal satellite imageries are used to extract the vegetation index of the whole province for a period between 1975 up to 2003 in depending upon the availability of satellite images.

Material and methods

Used data

Satellite Images - Four Landsat images (1MSS, 1TM and 2 ETM+7 acquired respectively in November 1975, November 1989, September and November 2001) and three scenes of ASTER images (one in September 2002 and two in November 2003) were obtained for the study areas. The tables 1 and 2 present Landsat and ASTER data specifications respectively.

Ancillary data are supplied by administrative maps of Thai Binh and statistic yearbook on fertilizer consumption of Thai Binh

Table 1: *Specification of Landsat data*

Aquired in Dec. 1975 (Landsat MSS)			
Band number & wavelength (micro-meter)	***VNIR (Visible & Near Infrared)***	***SWIR (Short Wave Infrared)***	***TIR (Thermal Infrared)***
	Band 4 (Green): 0.50~0.60	*Band 7: 0.9~1.1*	
	Band 5 (Red): 0.6~0.7		
	Band 6: 0.7~0.9		
Spatial Resolution	*57m * 79m*	*57m * 79m*	*Nil*
Swath width	*185 km*		
Acquired in Nov. 1989 (Landsat TM) and Sep. 2001, Nov. 2001 (Landsat ETM+7)			
Band number & wavelength (micro-meter)	***VNIR (Visible & Near Infrared)***	***SWIR (Short Wave Infrared)***	***TIR (Thermal Infrared)***
	Band 1 (Blue): 0.45~0.52	*Band 5: 1.55~1.75*	*Band 6: 10.4~ 12.5*
	Band 2 (Green): 0.52~0.6	*Band 7: 2.08~ 2.35*	
	Band 3 (Red): 0.63~ 0.69		
	Band 4 (NIR): 0.76~ 0.9		
	Panchromatic (ETM+): 0.52~ 0.9		
Spatial Resolution	*30 m (Pan: 15m)*	*30m*	*120 m (ETM+7: 60m)*
Swath width	*185 km*		
Revisited Frequency	*16 days*		

Table 2: *Specification of ASTER (Advanced Spaceborne Thermal Emission and Reflectance Radiometer) data*

Acquired in Nov.2003			
Band number & wavelength (micro-meter)	***VNIR (Visible & Near Infrared)***	***SWIR (Short Wave Infrared)***	***TIR (Thermal Infrared)***
	Band 1 (Green): 0.52~0.60	*Band 4: 1.600~1.700*	*Band 10: 8.125~8.475*
	Band 2 (Red): 0.63~0.69	*Band 5: 2.145~2.185*	*Band 11: 8.475~8.825*
	Band 3N (NIR): 0.76~0.86	*Band 6: 2.185~2.225*	*Band 12: 8.925~9.275*
		Band 7: 2.235~2.285	*Band 13: 10.25~10.95*
		Band 8: 2.295~2.365	*Band 14: 10.95~11.65*
		Band 9: 2.360~2.430	
Spatial Resolution	*15m*	*30m*	*90m*
Swath width	*60 km*		
Revisited Frequency	*16 days*		

Method

Image pre-processing

Considering the available images of Thai Binh are of different acquisition dates and are acquired by different sensors (MSS, TM, +ETM and ASTER) the radiometric and geometric corrections are needed in pre-processing procedures. Data providers and all the Digital Numbers were already converted into reflectance values of 32 bits by Radiometric Calibration. Geometric Correction was carried out by polynomial model using UTM WGS 84 projection. The details of Ground Control Point GCP and Root Mean Square RMS are presented in the table 3.

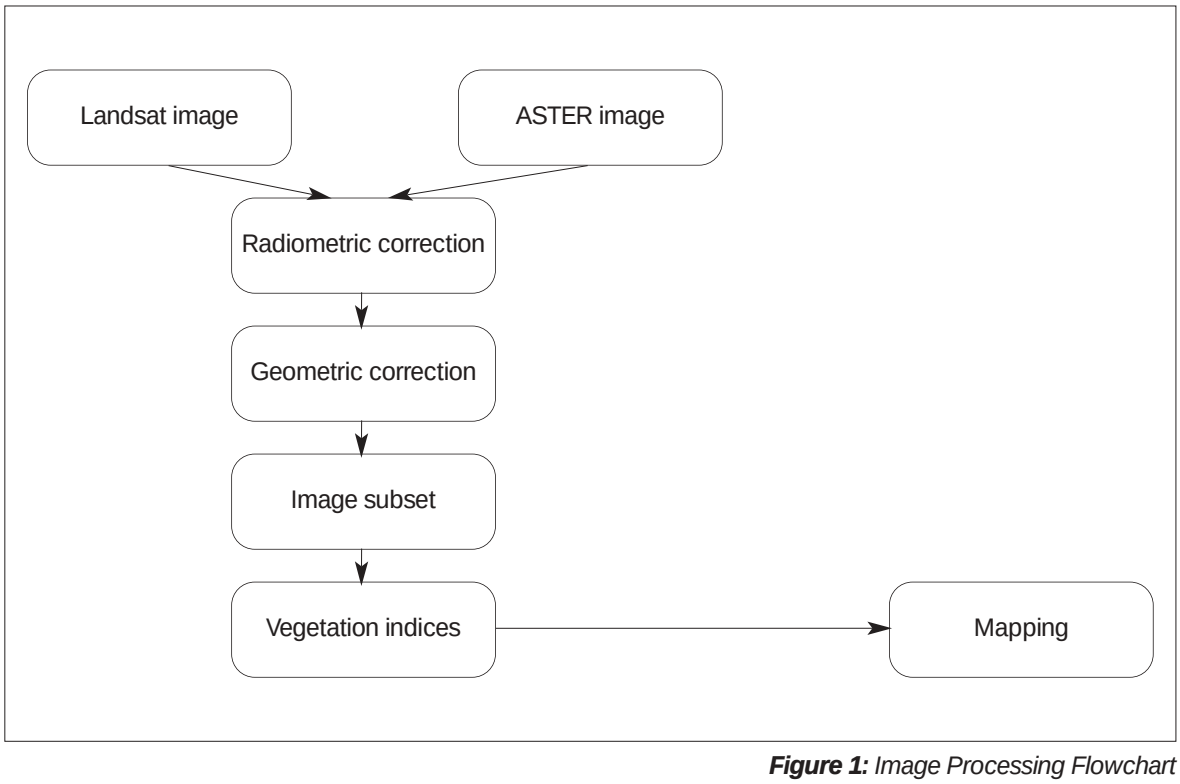

Figure 1: *Image Processing Flowchart*

Table 3: *GCP used for geometric correction of ASTER image 2003, 29 November scene 1*

ASTER image 2003, 29 November (scene 1) RMS Error: (0.29; 0.35)				
ID	***Uncorrected X***	***Uncorrected Y***	***Georeferenced X***	***Georeferenced Y***
1	*4287.1875*	*804.9375*	*636520.625*	*2248851.875*
2	*2904.9375*	*1563.8125*	*614310.625*	*2240731.875*
3	*3902.3125*	*1515.4375*	*629209.375*	*2239180.625*
4	*3587.4375*	*121.6875*	*627693.125*	*2260571.875*
5	*2292.5625*	*236.4375*	*608236.875*	*2261784.375*
6	*3219.59375*	*914.84375*	*620444.375*	*2249639.375*
7	*3491.5625*	*1975.3125*	*622079.375*	*2233301.875*
8	*2202.34375*	*1178.59375*	*604769.375*	*2248030.625*
9	*2814.8125*	*784.5625*	*614729.375*	*2252489.375*
10	*4138.5625*	*2029.5625*	*631545.625*	*2231028.125*
11	*4634.03125*	*76.96875*	*643318.125*	*2258855.625*
12	*2072.3125*	*2055.1875*	*600855.625*	*2235323.125*

Table 4: *GCP used for geometric correction of ASTER image 2003, 29 November scene 2*

ASTER image 2003, 29 November (scene 2) RMS Error: (0.25; 0.28)				
ID	***Uncorrected X***	***Uncorrected Y***	***Georeferenced X***	***Georeferenced Y***
1	*3488.4375*	*2228.4375*	*634396.875*	*2288654.375*
2	*2429.1875*	*2806.0625*	*617391.875*	*2282468.125*
3	*4128.0625*	*3880.6875*	*640151.25*	*2262701.25*
4	*2139.6875*	*3861.9375*	*610714.375*	*2267474.375*
5	*2005.4375*	*2158.4375*	*612559.0625*	*2293037.187*
6	*4484.84375*	*2685.03125*	*648144.6875*	*2279624.063*
7	*3466.40625*	*3274.40625*	*631710.3125*	*2273184.063*
8	*2909.03125*	*4104.09375*	*621576.875*	*2262146.875*
9	*4404.5625*	*3158.9375*	*645885.9375*	*2272780.938*
10	*3744.09375*	*3915.34375*	*634380.9375*	*2263057.812*

Table 5: *GCP used for geometric correction of ASTER image 31 August 2002*

ASTER image 13 August 2002 RMS Error: 0.20; 0.31				
ID	***Uncorrected X***	***Uncorrected Y***	***Georeferenced X***	***Georeferenced Y***
1	*1915.28125*	*2578.40625*	*632406.875*	*2247664.375*
2	*481.3125*	*3408.4375*	*609350.625*	*2238390.625*
3	*3545.5625*	*106.4375*	*661860.625*	*2280903.125*
4	*731.15625*	*155.28125*	*619967.8125*	*2286165.313*
5	*3965.8125*	*1569.0625*	*665000.625*	*2258289.375*
6	*2655.0625*	*3431.6875*	*641588.125*	*2233423.125*
7	*490.6875*	*1791.4375*	*612916.875*	*2262390.625*
8	*2239.4375*	*1124.4375*	*640308.125*	*2268563.125*
9	*2022.1875*	*157.0625*	*639130.625*	*2283391.875*
10	*1326.9375*	*878.9375*	*627284.375*	*2274159.375*
11	*3791.9375*	*2505.5625*	*660423.125*	*2244756.875*
12	*1034.5625*	*2363.8125*	*619779.375*	*2252731.875*
13	*2699.5625*	*2023.1875*	*645225.625*	*2254240.625*
14	*3637.098388*	*647.855779*	*662071.875*	*2272668.125*
15	*1542.6875*	*3663.6875*	*624570.625*	*2232346.875*

Table 6: *GCP used for geometric correction of Landsat image +ETM November 2001*

Landsat image November 2001 RMS error: (0.34, 0.38)				
ID	***Uncorrected X***	***Uncorrected Y***	***Georeferenced X***	***Georeferenced Y***
1	*912.0625*	*1054.1875*	*641173.75*	*2263341.25*
2	*1646.9375*	*438.5625*	*662111.25*	*2280911.25*
3	*104.8125*	*299.9375*	*618146.25*	*2284841.25*
4	*811.375*	*289.375*	*638271.25*	*2285158.75*
5	*1733.5625*	*1321.5625*	*664588.75*	*2255743.75*
6	*467.4375*	*834.0625*	*628505.625*	*2269595.625*
7	*1371.3125*	*1584.6875*	*654289.375*	*2248229.375*
8	*1698.0625*	*959.4375*	*663594.375*	*2266059.375*
9	*1063.9375*	*510.1875*	*645489.375*	*2278854.375*
10	*416.3125*	*510.4375*	*627029.375*	*2278843.125*
11	*1328.3125*	*1054.9375*	*653038.75*	*2263318.75*
12	*448.9375*	*1152.9375*	*627991.25*	*2260541.25*

Table 7: *GCP used for geometric correction of Landsat image +ETM September 2001*

Landsat September 2001 RMS error: (0.37, 0.58)				
ID	***Uncorrected X***	***Uncorrected Y***	***Georeferenced X***	***Georeferenced Y***
1	*840.1875*	*1368.8125*	*639113.75*	*2254381.25*
2	*413.3125*	*372.8125*	*626908.75*	*2282751.25*
3	*913.3125*	*1053.4375*	*641172.5*	*2263347.5*
4	*976.625*	*235.875*	*642951.25*	*2286676.25*
5	*1765.4375*	*1060.6875*	*665473.125*	*2263166.875*
6	*95.625*	*337.625*	*617856.25*	*2283783.75*
7	*358.1875*	*857.6875*	*625373.75*	*2268961.25*

Table 8: *GCP used for geometric correction of Landsat image TM November 1989*

Landsat image November 2001 RMS error: (0.34, 0.38)				
ID	***Uncorrected X***	***Uncorrected Y***	***Georeferenced X***	***Georeferenced Y***
1	*1535.3125*	*723.5625*	*658914.375*	*2272774.375*
2	*869.625*	*1158.125*	*639928.75*	*2260398.75*
3	*551.3125*	*117.9375*	*630845.625*	*2290039.375*
4	*631.1875*	*1428.6875*	*633108.75*	*2252686.25*
5	*681.3125*	*733.1875*	*634552.1995*	*2272502.24*
6	*1473.3125*	*1597.6875*	*657145.625*	*2247836.875*
7	*1768.3125*	*983.3125*	*665553.75*	*2265378.75*
8	*426.3125*	*674.9375*	*627281.875*	*2274161.875*
9	*1244.8125*	*727.3125*	*650619.375*	*2272665.625*
10	*1127.6875*	*1158.5625*	*647295.625*	*2260375.625*
11	*1210.3125*	*296.6875*	*649641.875*	*2284950.625*
12	*440.8125*	*1151.6875*	*627696.25*	*2260571.25*

Table 9: *GCP used for geometric correction of Landsat image MSS December 1975*

Landsat December 1975 RMS error: (0.41, 0.50)				
ID	***Uncorrected X***	***Uncorrected Y***	***Georeferenced X***	***Georeferenced Y***
1	*857.875*	*1132.375*	*639605.625*	*2261036.875*
2	*636.625*	*701.875*	*633274.375*	*2273323.125*
3	*1153.625*	*556.625*	*647997.5*	*2277472.5*
4	*80.875*	*379.625*	*617393.75*	*2282466.25*
5	*1106.375*	*1288.125*	*646698.125*	*2256586.875*
6	*1745.625*	*898.875*	*664921.875*	*2267711.875*
7	*1213.875*	*923.375*	*649768.125*	*2267011.875*

Index Computing

Vegetation index (VI) is one of the physical indices we can compute from the spectral bands of remote sensing image. The vegetation index VI is used in different applications such as canopy and biomass estimation, crop monitoring and drought monitoring etc. In the literature, other VI are cited and differ in terms of spectral bands and the algorithms and in terms of application (Rouse et al 1974; Colwell et Suits 1975; Huete, 1988; Richardson and Wiegand 1977; Baret et al. 1989; Kaufman et Tanré, 1992 ; Qi et al 1994). The paragraphs bellow describe some of these indices used for our study.

SAVI (Soil Adjusted Vegetation Index) computes the ratio between red and near infrared spectral region with some added terms to adjust for different brightness of background soil (Huete, 1988). Due to paddy

harvested time ends in October, the result of SAVI images during November-December presents the situation of natural vegetation in the province. The SAVI image of September helps to understand the agricultural activities in details. The Normalized Differential Water Index (NDWI) estimates the situation of water in the province. The ratio between red and Short Wave Infrared (SWIR) spectral region clearly enhanced water bodies to the brighter pixels (CPM, 2003).

$$SAVI = \left[\left(\frac{\rho_{nir} - \rho_{red} + L}{\rho_{nir} + \rho_{red}} \right) \times (1 + L) \right] + 1$$

Where: *p* is the reflectance, L~ 0.5

$$NDWI = \left[\frac{\rho_{red} - \rho_{swir}}{\rho_{red} + \rho_{swir}} \right] + 1$$

Bare Soil Index (BI) was also computed to identify difference between agriculture and none agriculture vegetation. The bare soil, fallow lands, and vegetation (with marked background response) are enhanced when using the BI index (Jamalabad and Abkar, 2004).

$$BI = \frac{(\rho_{swir} + \rho_{red}) - (\rho_{nir} + \rho_{blue})}{(\rho_{swir} + \rho_{red}) - (\rho_{nir} + \rho_{blue})} + 1$$

As for 2003, the non-vegetation objects are additionally extracted from Urban Index UI (Kawamura, M., S. Jayamamana and Y. Tsujiko 1997) to emphasize the vegetation presence and UI is very helpful to discriminate vegetation and non-vegetation land cover types. The UI is calculated as following:

$$UI = \frac{(\rho_{swir2} - \rho_{red})}{(\rho_{swir2} + \rho_{red})} + 1$$

For Landsat MSS, we compute p_{nir} from band 3 and p_{red} from band 2. For Landsat TM and ETM+, p_{nir} is computed from band 4, p_{red} from band 3, p_{swir} from band 5 and p_{swir2} from band 7, p_{blue} from band 1. For ASTER, p_{red}, p_{nir}, p_{swir} , p_{swir2} are taken from band 2, 3, band 4, band 5 respectively. All the equations above provide value ranges from -1 to +1. To avoid negative value in further analysis, we have added +1 in each equation. Thus, the resulted images will have value between 0~2 where higher value show the existence of the environment parameters (i.e. high in SAVI shows high in vegetation, high in NDWI shows high in water). We compute also mean and standard deviation from each index at commune level to analyze the environmental situation with socio-economic condition at each commune.

Scaling problem and solution

As explained in previous sector of this report, due to the difference of acquisition dates and especially, to the spectral band difference, the VI values computed for ASTER images vary between 0.80131286 and 1.18813098 meanwhile the range of VI computed for Landsat images is in between 0.64208417 and 1.09550542. In order to compare these values we need to scale the ASTER VI values to fit the Landsat VI range using relative scaling method. This method is described by the formula:

$$N = n * \delta + \alpha$$

Where:

$$\delta = \frac{x_{\max} - x_{\min}}{X_{\max} - X_{\min}}$$

And

$$\alpha = X_{\min} / \delta - x_{\min}$$

Where:

- N: Grey level value after calibration
- n: Orginal grey level value to be calibrated
- δ: Stretching co-efficient for the set of pixel to be calibrated
- α: Shifted co-efficient for each pixel
- X_{max} Maximum grey level value of pixels in the standard image
- X_{min} Minimum grey level value of pixels in the standard image
- x_{max}: Maximum grey level value of pixels in the dependent image
- x_{min}: Minimum grey level value of pixels in the dependent image

In this study, we used the value extracted from the image Landsat ETM+7 acquired in November 2001 as the reference.

Results

Multidate statistical variations of indices

SAVI, BI, NDWI and UI indices were computed in multi-temporal Landsat images and ASTER images (see fig. 2.1 to 2.19). The multidate statistical variations of computed indices are used to analyze the environmental changes with respect to vegetation, agriculture, water and urban activities. The indices after calibration have produced relative results based on electromagnetic spectrum recorded in the images. The mean score and coefficient of standard deviation of each index were carefully evaluated at commune level. Standard deviation of mean helped to understand the distribution pattern of the objects in the land surface.

Principally, the SAVI appears brighter in healthy vegetation areas whereas BI seems brighter in bare land areas. The high NDWI corresponds to the areas with high water content. The variation of UI index indicates the different density of urban and built areas.

The SAVI index of 1975, 1989, 2001, 2003 represent the natural vegetation coverage in brighter areas. It is because of seasonal variance in agriculture practice. The high content of chlorophyll can be observed in paddy field in September. The paddy harvest is completed at the end of October. Therefore, harvested paddy fields on the images taken during November and December have a high bare soil index BI and appear in brighter pixels.

Some inconsistencies in distribution pattern of the mean of SAVI are observed in some communes. Decreasing trend of natural vegetation is observed in past three Bare soil index of 2001 is also getting lower as compared to year 1989. Mean distribution of the bare soil index seems more consistent as compared to SAVI mean. Comparison of BI with SAVI makes sense of conventional agriculture occupancy as well as practices. There are not so much fluctuations in distribution of objects in BI. Decreasing patterns in SAVI and BI exposed the decreasing of conventional agriculture practices (i.e. paddy).

The result of NDWI is quite different than SAVI and BI. Increasing pattern is observed in water bodies although inconsistency in distribution of the water bodies is found in some communes.

Several farmers in the province are changing their traditional agriculture land to modern aquatic practices. It is one of the major factors that increased the water properties and reduced the vegetation properties as compared to 1980s. Direct relation of fish farms to the pig production was observed during the field visit. Pig waste is being used as a source of input for aquatic farming fertilization of ponds, nutrient for fishes. Thanks to the high demand of lean pork meat in the growing cities and flexible government policies, farmers are attracted to the integrated agriculture practices (pig and fish ponds).

There is very good compromise between water and urban index. Most of the urban areas are observed along the water bodies like rivers, canals and lakes. The increased urban activities in the province do not have significant impact in reducing water properties. But it has significant impact in reducing the vegetation. The UI mean increased as a peak in some communes whereas the SAVI mean decreased just like a gorge in the corresponding communes. So, the land of agriculture is being occupied by urban function. The conversion of agriculture land to urban uses is natural economic process in widely observed in Thai Binh.

Relation between vegetation activities and urban function was checked in September 2001 results and found correlation coefficient at -0.606. It has strong negative linear relation between the UI and SAVI mean, which suggest the urban activities replacing the natural environment significantly.

Vegetation is thus getting sparse day by day because of growing urban activities, integrated agriculture practices, government priorities on intensification of pig production and aquatic products.

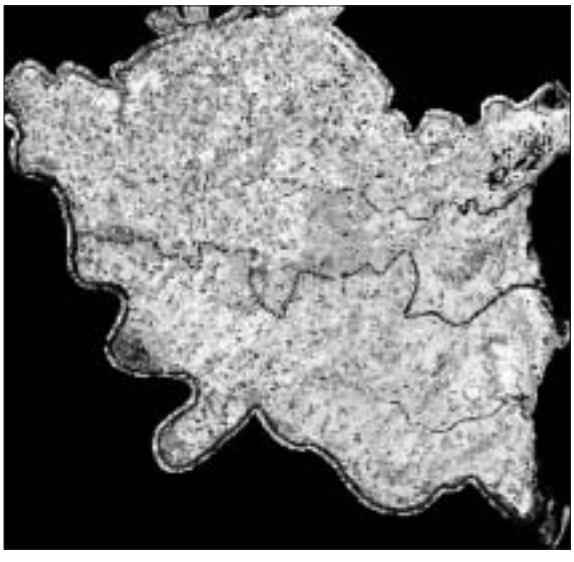

Figure 2.1: *Bare soil index in 1989*

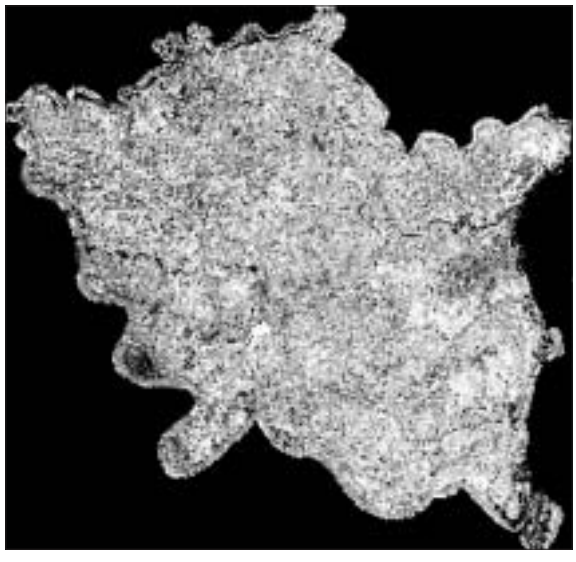

Figure 2.2: *Bare soil index in 2001*

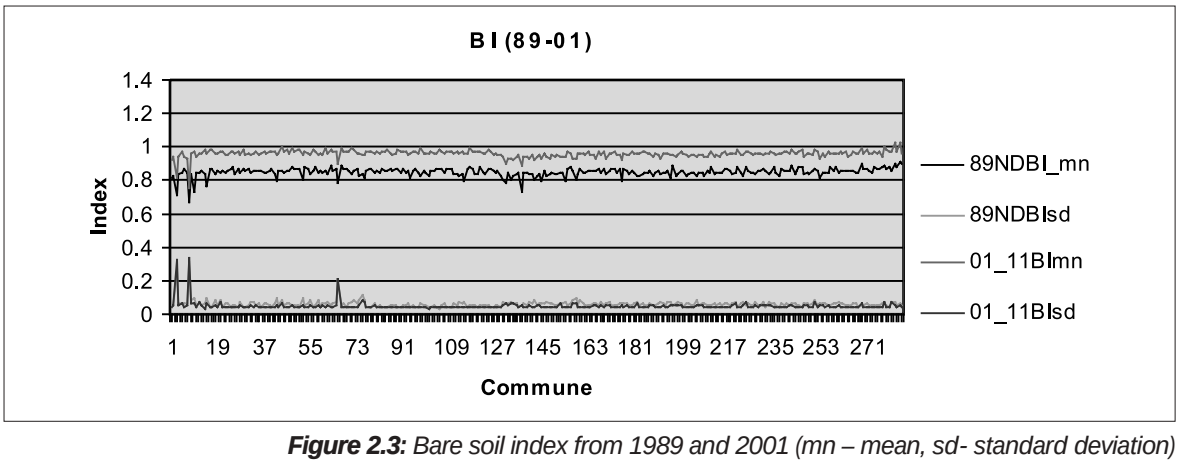

Figure 2.3: *Bare soil index from 1989 and 2001 (mn – mean, sd- standard deviation)*

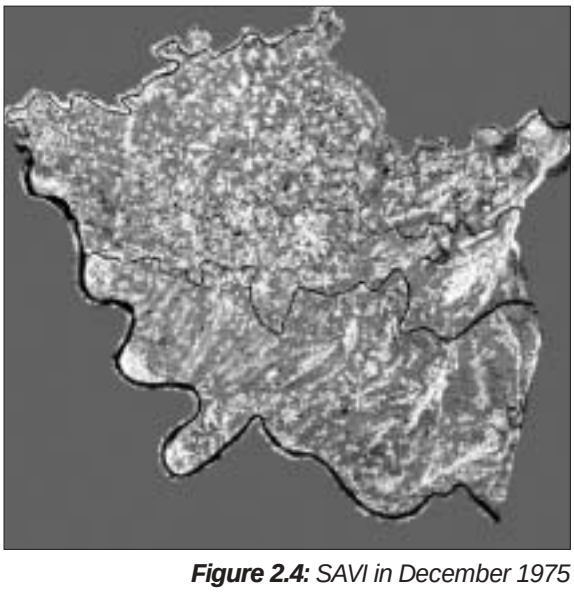

Figure 2.4: *SAVI in December 1975*

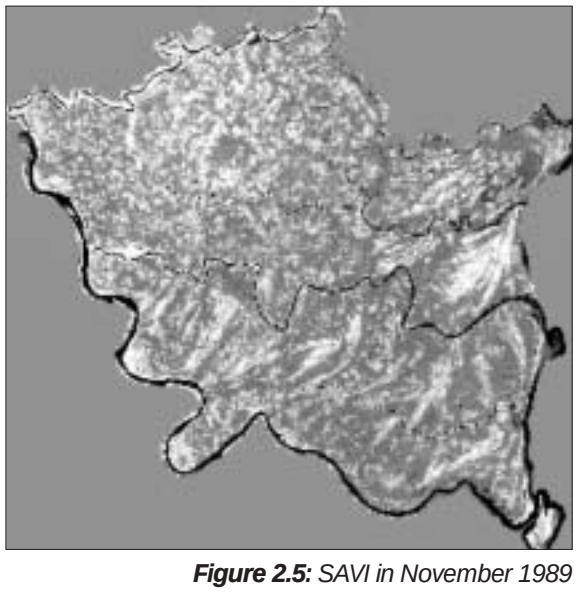

Figure 2.5: *SAVI in November 1989*

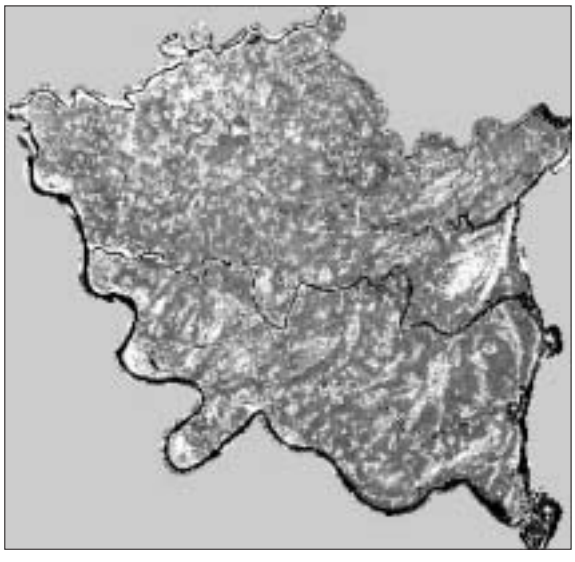

Figure 2.6: *SAVI in 2001, November*

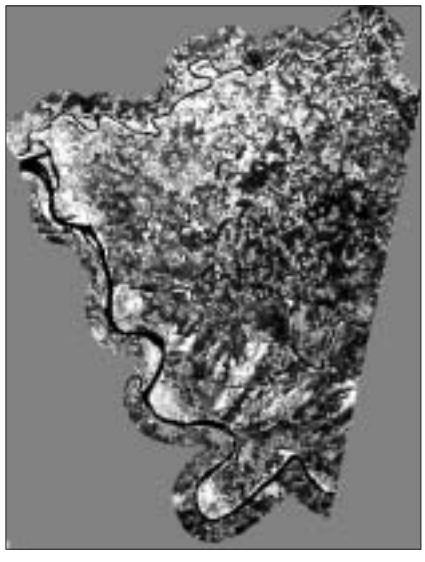

Figure 2.7: *SAVI in November 2003*

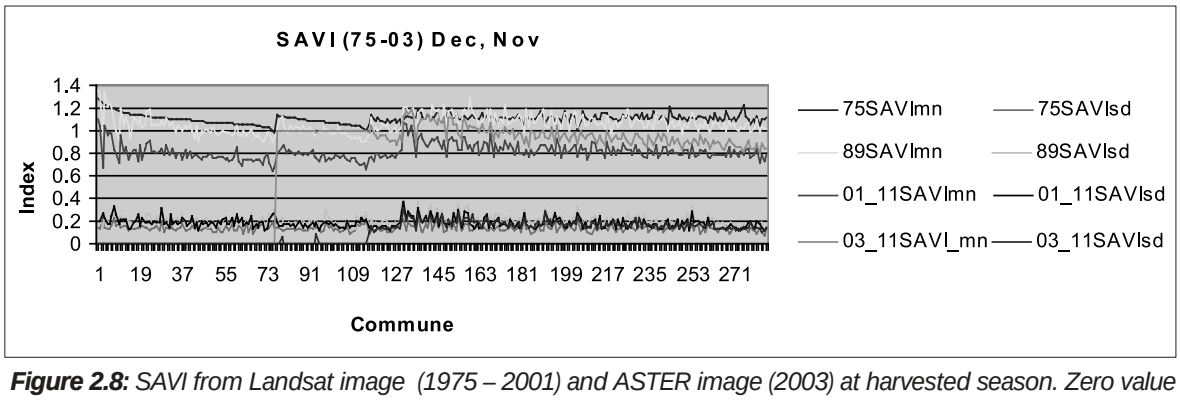

Figure 2.8: *SAVI from Landsat image (1975 – 2001) and ASTER image (2003) at harvested season. Zero value is considered for communes from 1 to 116 due to the lack of image (mn- mean, sd-standard deviation)*

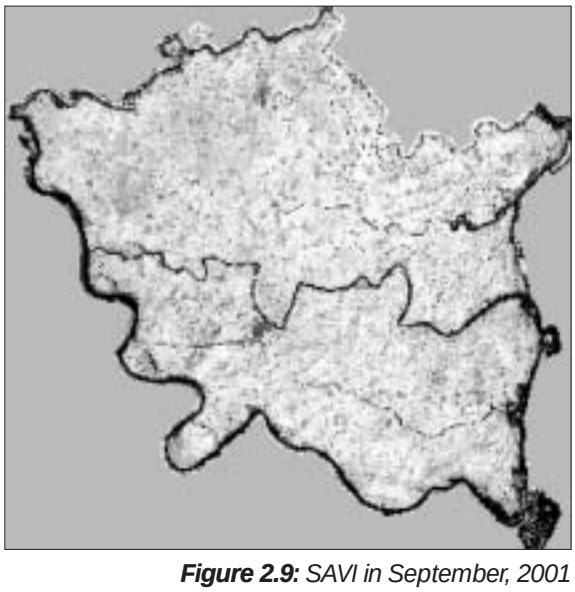

Figure 2.9: *SAVI in September, 2001*

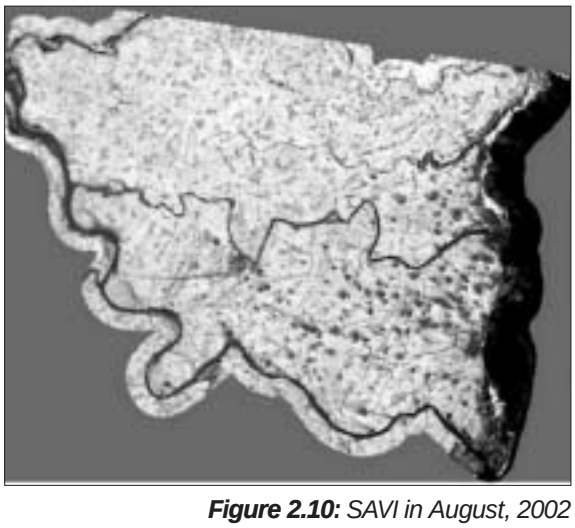

Figure 2.10: *SAVI in August, 2002*

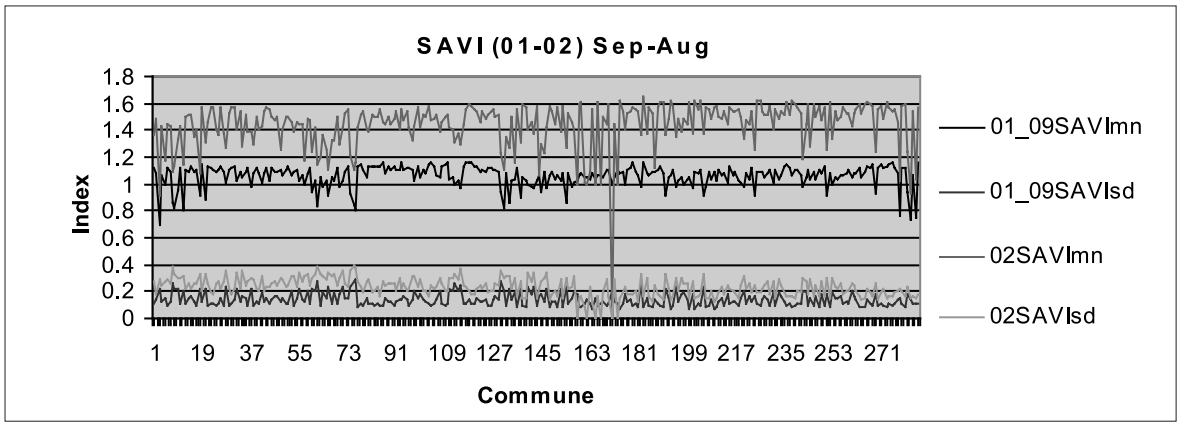

Figure 2.11: *SAVI in farming season taken from Landsat image and ASTER image. The SAVI values from ASTER image are particularly high due to influence of cloud (mn- mean, sd- standard deviation)*

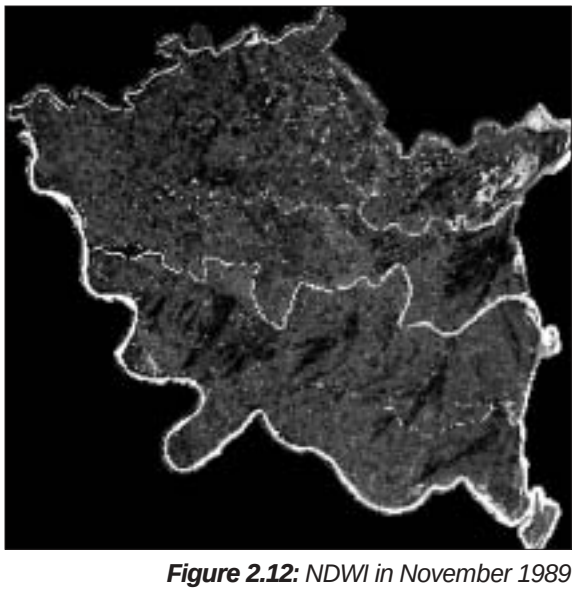

Figure 2.12: *NDWI in November 1989*

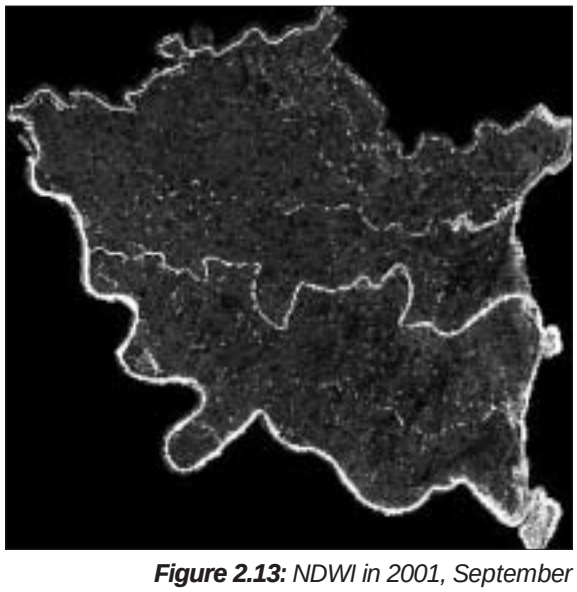

Figure 2.13: *NDWI in 2001, September*

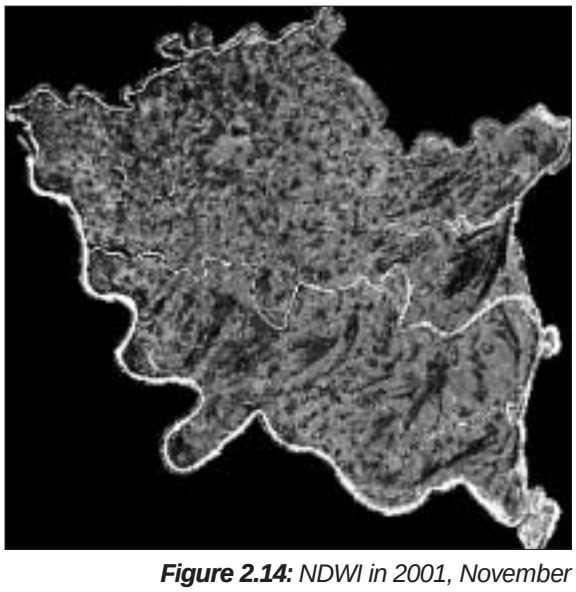

Figure 2.14: *NDWI in 2001, November*

Figure 2.15: *NDWI in November 2003*

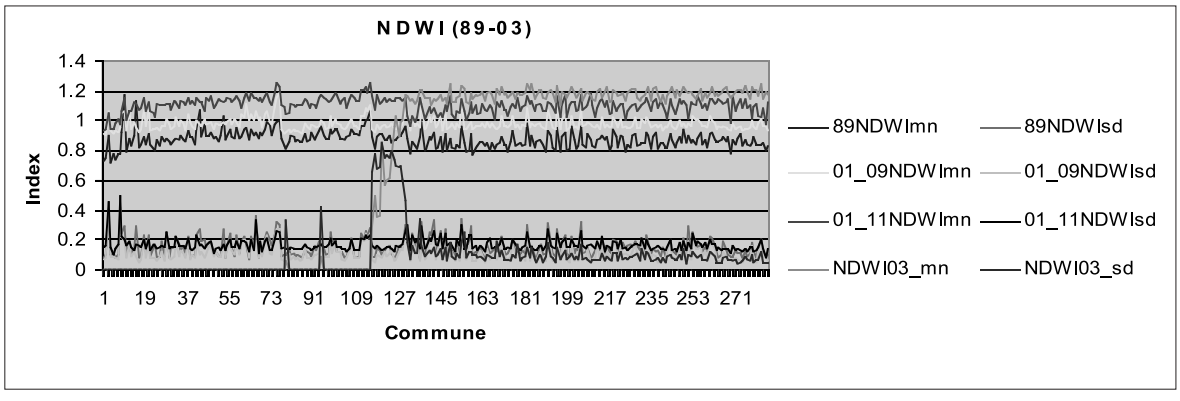

Figure 2.16: *NDWI from 1989 to 2003. NDWI from 2003 is considered 0 for 1st -116th ordered communes owing to the lack of image covering them (mn-mean, sd- standard deviation)*

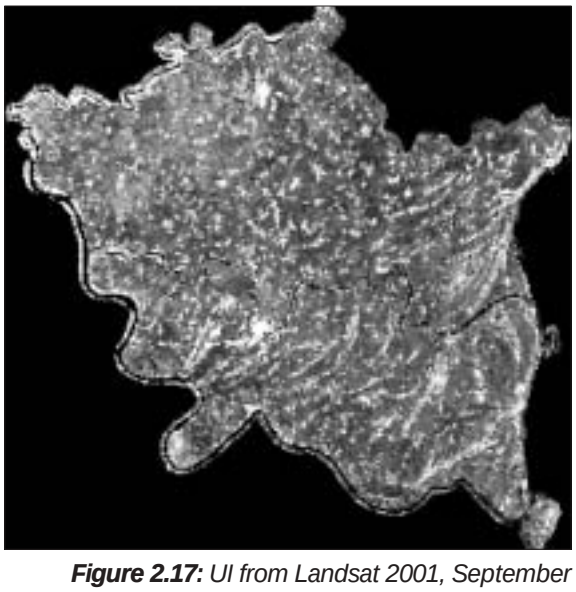

Figure 2.17: *UI from Landsat 2001, September*

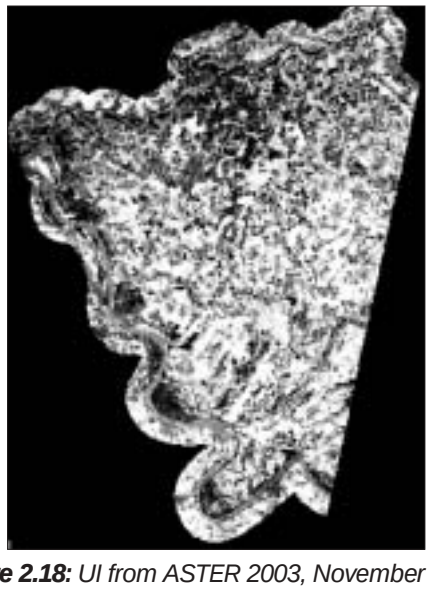

Figure 2.18: *UI from ASTER 2003, November*

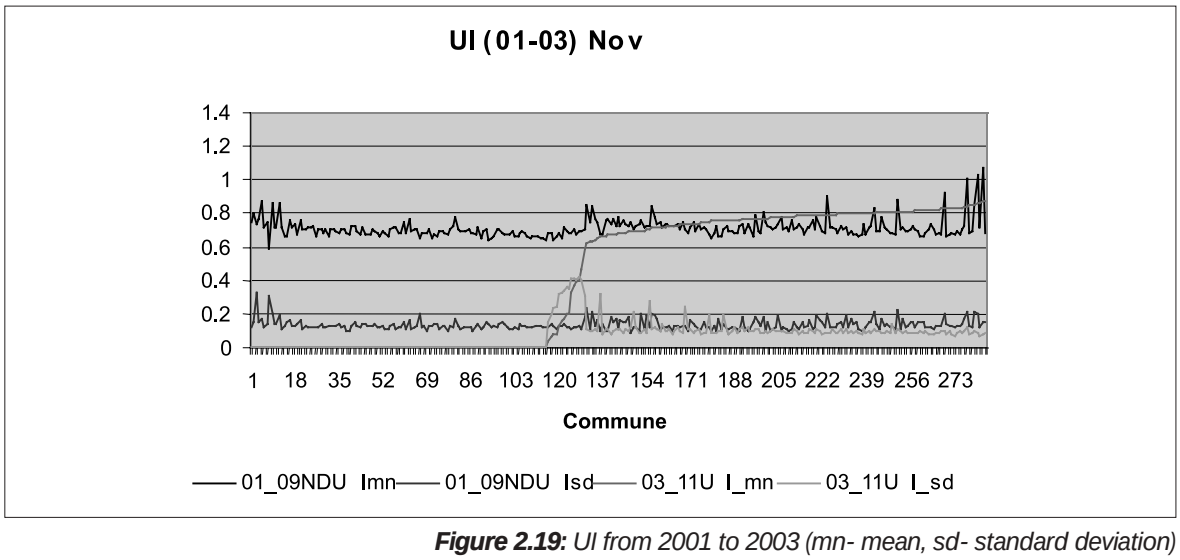

Figure 2.19: *UI from 2001 to 2003 (mn- mean, sd- standard deviation)*

Cartographic Representation of results

Due to the limits in statistic data, we cannot make a full representation of all physical index. The geo-referenced index images are crossed with the administrative map of Thai Binh to produce the normalized biophysical indices map at communal level, i.e., each commune of Thai Binh is now characterized by a series of Vegetation Index. The results are presented in a cartographic database of which the attribute data describing the computed indices are organized in relational model and very easy to manipulate in GIS environment.

Mean SAVI (Soil Adjusted Vegetation Index) Map by Commune

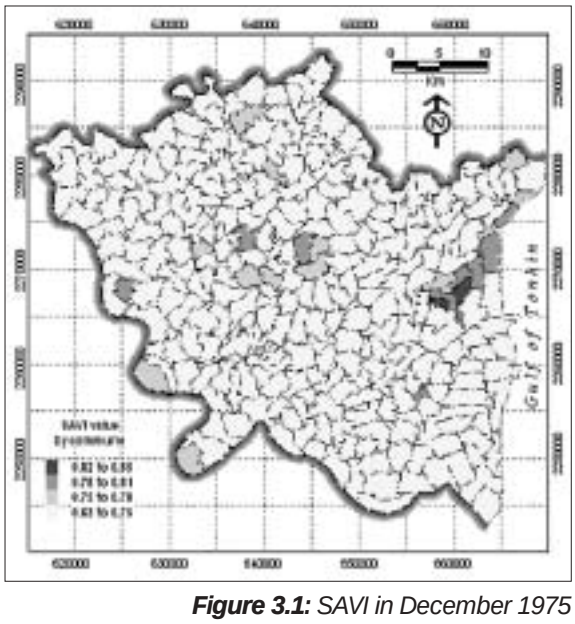

Figure 3.1: *SAVI in December 1975*

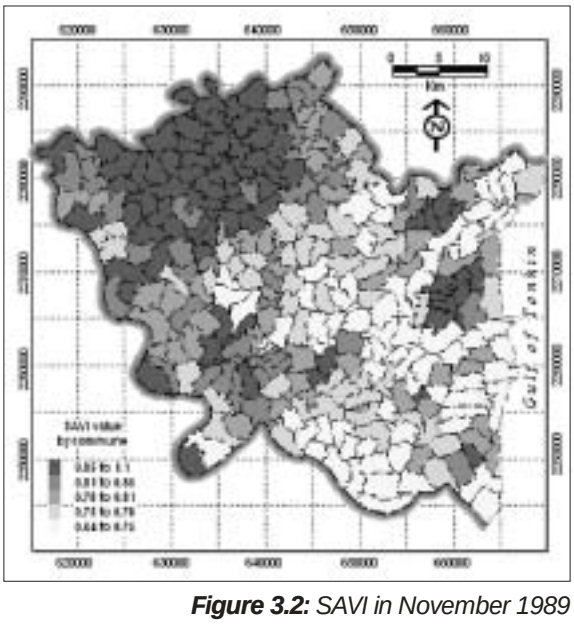

Figure 3.2: *SAVI in November 1989*

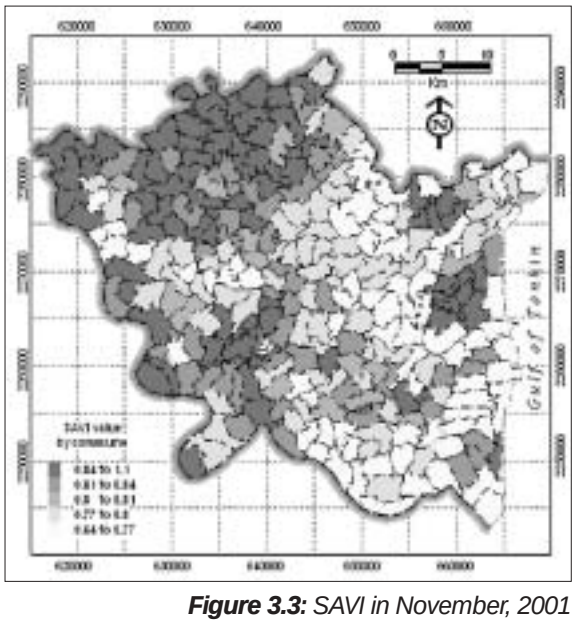

Figure 3.3: *SAVI in November, 2001*

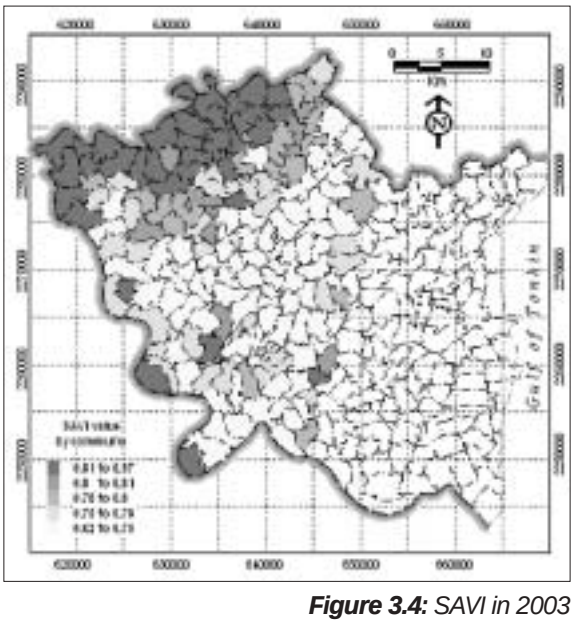

Figure 3.4: *SAVI in 2003*

The SAVIs are extracted from Landsat and ASTER data, which were acquired during the harvesting season (Novembers). To facilitate the analysis, the SAVI mean values are associated to each commune and this value represents mean SAVI of the whole communal territory. As mentioned above, the scaling of SAVI values of the two dates of Landsat and ASTER data allows comparisons each with other. The higher communal SAVI the larger vegetation cover is (fig. 3). Due to its scene limitation, ASTER data covers only a part of Thai Binh and no value is computed for the non-data area.

As the Landsat and ASTER data are acquired in the period of similar climate conditions the atmospheric influence is negligible. The very low value of SAVI extracted from MSS data can be explained by its low spatial resolution (57m*79m) and bandwidths.

For the period from 1989 to 2003, the high SAVI values are concentrated in the Western and North West communes of Thai Binh even if the acquisition dates coincided to the harvest period. This phenomena may be explained by the presence of other cultures than rice in this period (for example vegetable, soya-bean etc.) which have been planted just after the harvest. To check this hypothesis, we used the statistic data on communal fertilizer consummation for winter plants and have found the high correlation between the consumption/use of fertilizer and SAVI values in these communes (Fig.4).

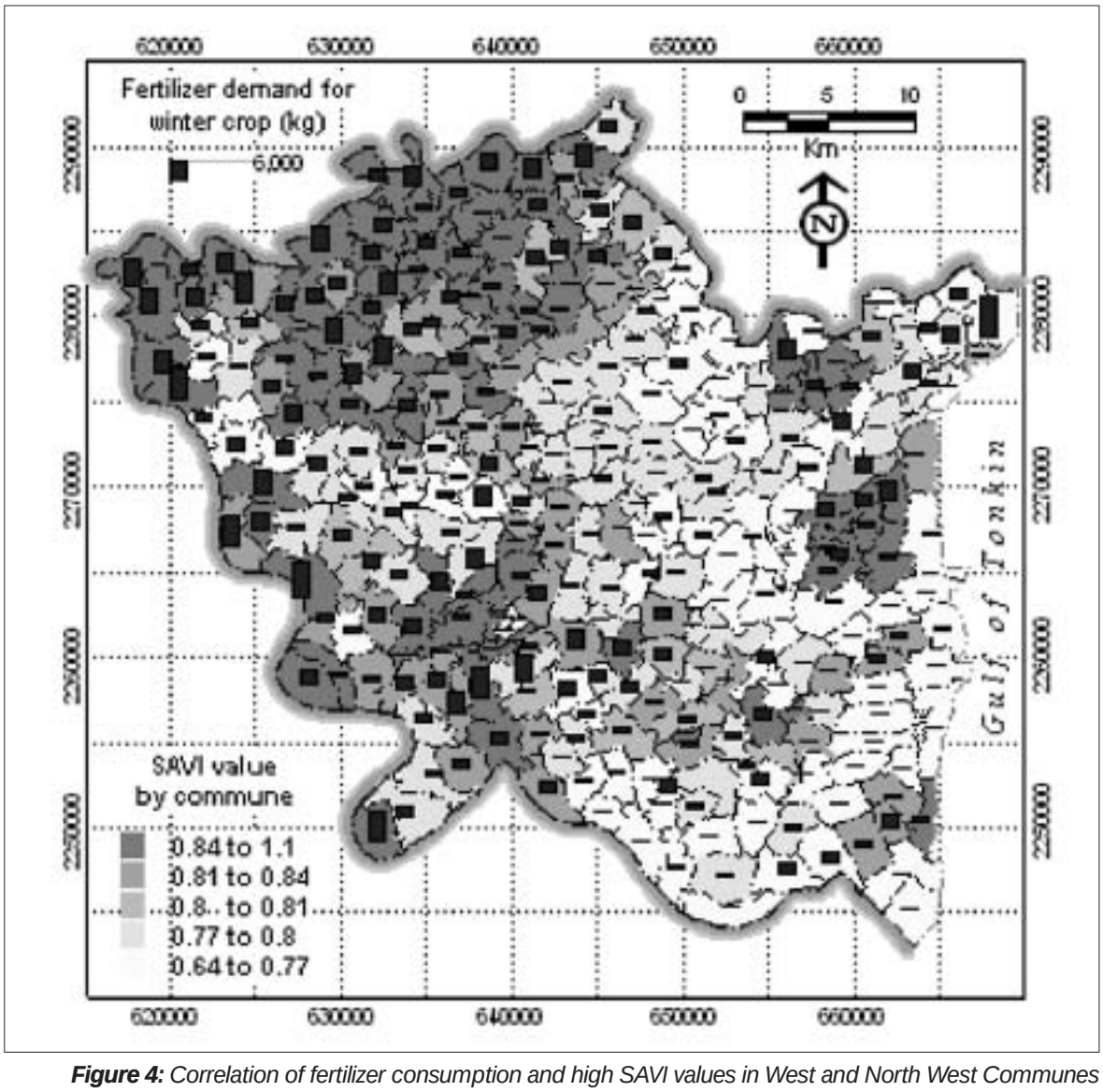

Figure 4: *Correlation of fertilizer consumption and high SAVI values in West and North West Communes*

Mean NDWI (Normalized Difference Water Index) Map by Commune

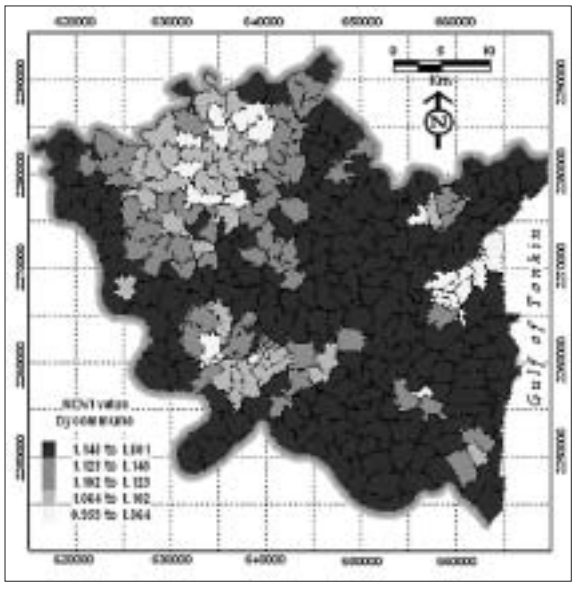

Figure 5.1: *NDWI in November 1989*

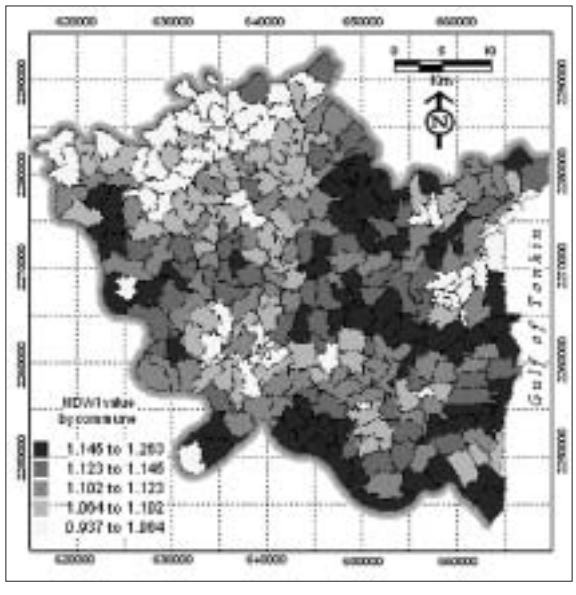

Figure 5.2: *NDWI in November, 2001*

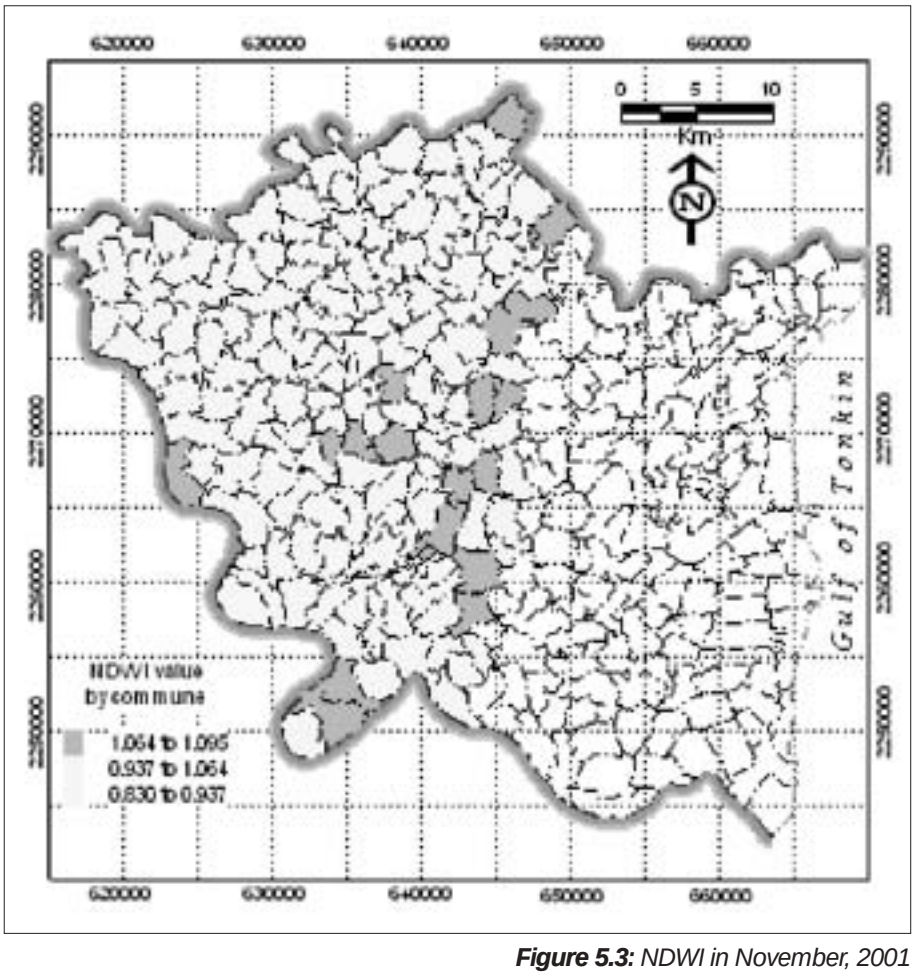

Figure 5.3: *NDWI in November, 2001*

NDWI was introduced by Gao (1996) to assess water content in a normalized way. This index increases with vegetation water content or from dry soil to free water. For the reference, we take the Land Use Map of 2000, the closest to Landsat image acquisition date we can have. The low NDWI values extracted from the Landsat TM and +ETM images acquired during dry season (November) of 1989 and 2001 indicate the low water content in soil and vegetation in the North West sector of the province. However, there observed a big difference in NDWI in the rest of territory in these two dates (Fig. 5.2, 5.3). This difference is thought related to the change of land use from rice in 1989 to Winter Crop in 2001.

The NDWI computed for ASTER image (Fig. 5.3) captured in November 2003 that covers only the West part of Thai Binh are low and corresponds to the area of Winter Crop.

In general, the NDWI values of North West Communes are lower than in other places (fig. 5.1 to 5.3) and showing the dryer soil conditions. In spite of that, their SAVI values indicate the existence of some vegetation (fig. 3.1 to 3.4) supposed to be winter vegetables as shown in Land Use Map (fig.7). These communes are mainly characterized by a high topography (see Chapter 2) and poorly irrigated terrain. Figure 6 shows the coincidence of winter crop and permanent vegetation (presented in black) with the areas of low NDWI values (between 0.937 and 1.102).

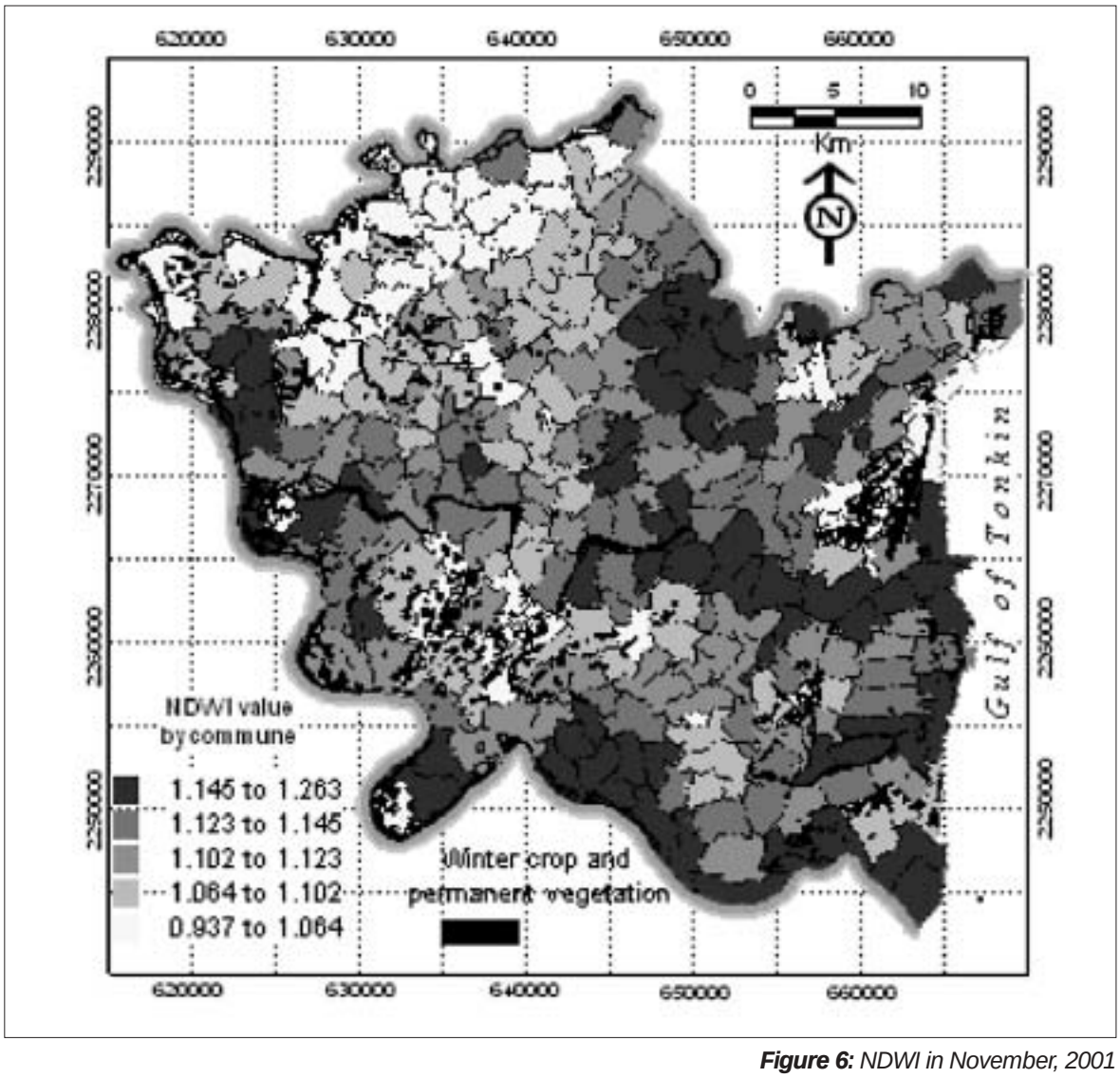

Figure 6: *NDWI in November, 2001*

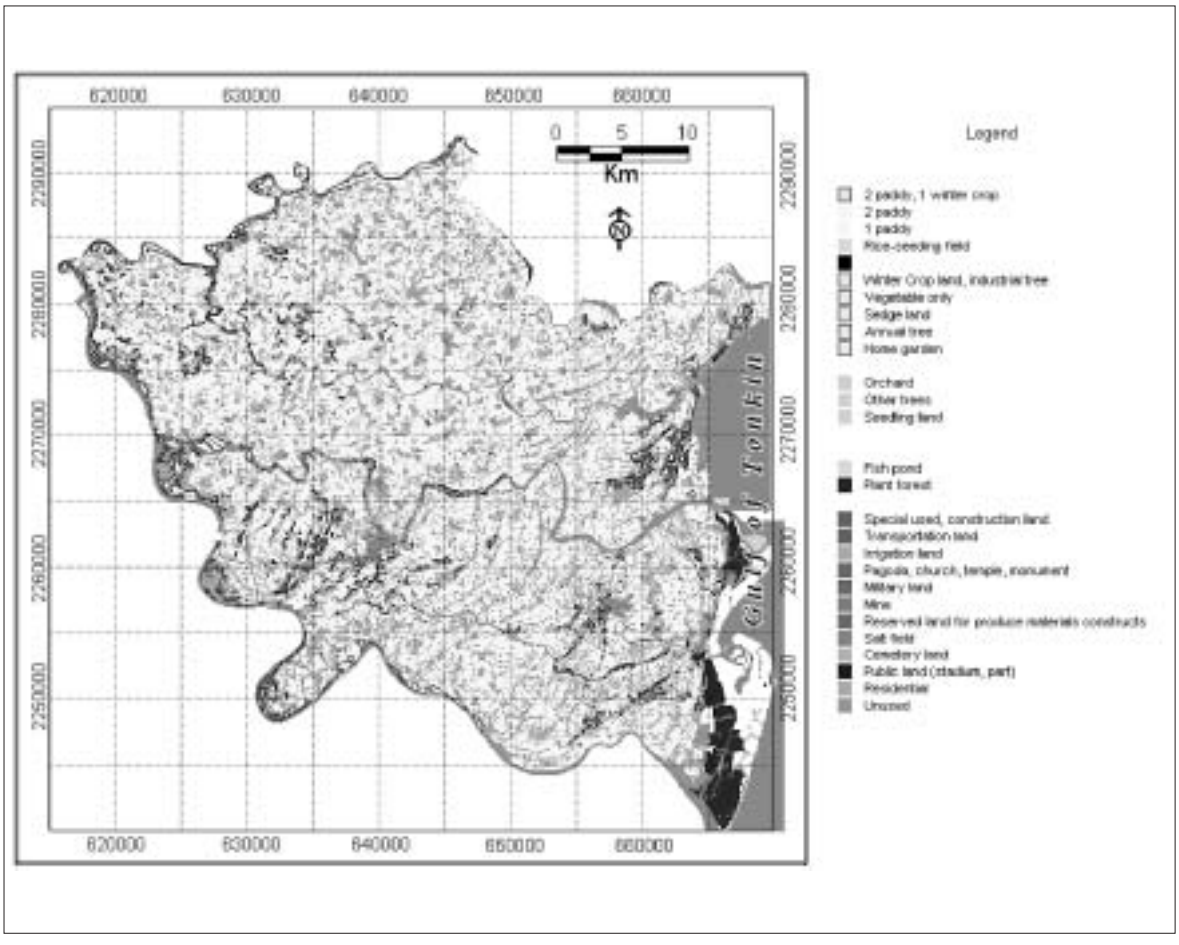

Figure 6: *Land use map of Thai Binh 2000 (Source Thai Binh Province)*

Conclusion

Different physical indices extracted from a time series of satellite images between 1975 and 2003 allow characterizing the changes of land cover in Thai Binh in this period. Based on SAVI, UI and BI indices change evaluation, the surface of winter crop appeared to decrease gradually and concentrate mainly in suburb communes of Thai Binh City and the adjacent communes of Vu Thu and Dong Hung Districts.

The communes having high NDWI (1.102~1.263) have been reduced in the period 1989-2003. The brutal decrease of NDWI scale computed for ASTER image have highlighted the difference in spatial and spectral resolution of this sensor; this is to be verified by ancillary statistic data.

Comparison between SAVI and NDWI values evaluated the spatial repartition of dry season land cover types; where the high SAVI values (0.8-1.1) coincide with low values of NDWI (0.937-1.102), we can observe the presence of winter crop. This inverse relation could be used to monitor the winter crop in dry season.

For the first time, we have found a good correlation between fertilizer demand statistics and high values of SAVI which indicate the high demand in fertilizer of North West communes where the winter crop are predominant in dry season.

The integration of SAVI, NDWI, UI and BI on the administrative map with communal boundaries of Thai Binh provides a good tool for spatial analysis of multi-temporal changes of land cover characteristics and for analyzing spatial correlation between these characteristics and other socio-economic data we may have in Thai Binh

References

1. Arbelo Rodríguez, C.D., A. Rodríguez Rodríguez, J.A. Guerra García and J.L. Mora Hernández, (2002), Soil Quality and Plant Succession in Forest Andosols, 12th ISCO Conference, Beijing, pp 452- 458.
2. Baret F.G., G. Guyot and D.-J. Major, 1989. A vegetation index which minimizes soil brightness effects on LAI and APAR estimation, 12th Canadian Symposium on Remote Sensing, Canadian Remote Sensing Society, Vancouver, p. 1355-1358.
3. Barnes, E.W., K.A. Sudduth, J.W. Hummel, S.M. Lesch, D.L. Corwin, C. Yang, C.S.T. Daughtry and W.C. Bausch (2003). Remote- and ground-based sensor techniques to map soil properties. Photogrammetric Engineering and Remote Sensing 69 619-630.
4. Colwell G.E. and G.H. Suits, 1975. Yield prediction by analysis of multispectral scanner data, NASA-CR 141865, ERIm 109600-17-F, NASA.
5. Huete, A.R., 1988. Asoil –adjusted vegetation index (SAVI), Remote Sensing of Environment, no 25, p.295-309.
6. Jamalabad, M. S. and A.A. Abkar (2004). Forest Canopy Density Monitoring, Using Satellite Images. XXth ISPRS Congress, Istanbul 12-23 July.
7. Kaufman, Y.-J. and D.-C. Tanré, 1992. Atmospherically Resistant Vegetation Index (ARVI) for EOS-MODIS, IEEE Transaction on Geoscience and Remote Sensing, vol. 30, no 2, p.261-270.
8. Kawamura, M., S. Jayamamana and Y. Tsujiko (1997). 'Comparison of Urbanization and Environmental Condition in Asian Cities using Satellite Remote Sensing Data'. Available online: http://www.gisdevelopment.net/aars/acrs/1997/ps1/ps2008.shtml [Downloaded: 12 January, 2006]
9. C. López-Fand, M.T. Pard, 2002, The impact of tillage systems and machinary traffic on some soil properties and crop yield in a calcic luvisol of central Spain, 12th ISCO Conference, Beijing, pp138-143.
10. Lunetta R.S. and C.D.Elvidge, (Editors), 1998, Remote Sensing Change Detection: Environmental Monitoring Methods and Applications, Ann Arbor Press, Michigan, 318 p.
11. Palacios-Orueta, A., J. E. Pinzon, D. A. Roberts, and S. L. Ustin. (1998). "emote sensing of soil properties in the Santa Monica Mountains: Hierarchical Foreground and Background Analysis." Seventh Annual JPL Airborne Earth Science Workshop, Pasadena, CA. January 12-16, 1998.
12. Qi J., A. Chenbouni, A.R. Huete, Y.H. Kerr and S. Soroonshian, 1994. A Modified Soil Adjusted Vegetation Index (MSAVI), Remote Sensing of Environement, no 48, p. 119-126.
13. Richardson, A. and C. Wiegand, 1977. Distinguishing vegetation from soil background information, Photogrametric Engineering and Remote Sensing. No 43, p.1522-1541.
14. Rouse, J.W., R.H. Haas, J.A. Schell, D.W. Deering and J.C. Harla, 1974. Monitoring the vernal advancement retrogradation (Green Wave Effect) of natural vegetation, Maryland, USANASA/GFSC, Greenbelt.
15. Smith, W.N., Desjardins, R.L., Grant, B. and Lemke, R., 2002, Estimated N2O Emissions as Influenced by Agricultural Practices in Canada, 12th ISCO Conference, Beijing 2002, pp 317- 323.
16. Uno, Y., Prasher, S.O., Patel, R.M., Strachan, I.B. and Pattey, E. 2005. Development of field-scale soil organic matter content estimation models in Eastern Canada using airborne hyperspectral imagery. Canadian Biosystems Engineering/Le génie des biosystèmes au Canada 47: 1.9 - 1.14